Aust. J. Phys., 1976, **29**, 419–33

A Search for Recombination Line Emission from the Galactic Equator at 408 MHz

M. J. Batty

The Chatterton Astrophysics Department, School of Physics, University of Sydney, N.S.W. 2006.

Abstract

A search for H 252α recombination line emission was made by scanning the galactic equator region using the Molonglo radio telescope. Upper limits were established over the range of galactic longitude accessible to the instrument. For the region $|l| \lesssim 40°$, estimates of the background thermal continuum brightness temperature were used to derive lower limits of $\sim$2000 K for the electron temperature of the gas along the line of sight. Lower limits for the electron density obtained by considering probable non-LTE effects suggest that the thermal emission over this range is due to low surface brightness HII regions. The observed H 252α upper limit averaged over the range $270° \lesssim l \lesssim 320°$ just admits the line intensity calculated by Shaver (1975) for the cold cloud component of the general interstellar medium.

1. Introduction

Recombination line emission has been observed at a number of positions near the galactic equator apparently free of discrete HII regions. First detected by Gottesman and Gordon (1970), this line emission appears to be confined to the region $|l| \lesssim 40°$ (Gordon *et al.* 1972; Matthews *et al.* 1973). Cesarsky and Cesarsky (1971) have argued that the line emission may originate in the cool cloud component of the interstellar medium, whilst most other workers have suggested regions with electron temperatures greater than 1000 K as the probable source (e.g. Jackson and Kerr 1971, 1975; Matthews *et al.* 1973; Hirabayashi 1974; Pankonin 1975). Electron temperatures in the range 1000–6000 K have been deduced for the line emitting medium by using various methods, but there is not yet total agreement about the nature of this medium, due to the difficulty in accurately determining the *continuum* thermal brightness temperatures. In addition, recent calculations by Shaver (1975) indicate the possibility of detecting strong recombination line emission near 100–200 MHz due to the effects of maser action in the cool component of the general interstellar medium. Radiation from strong continuum sources, or even the diffuse nonthermal galactic background, could be responsible for strong line enhancement under suitable conditions, and such effects could still be important at frequencies near 400 MHz.

Since relatively few recombination line observations of galactic sources have been made near 400 MHz, the major part of the galactic equator region has not been examined in any systematic manner, and thus even a low sensitivity search would be useful. It was hoped that the present investigation using the Molonglo radio telescope might provide some independent information in this area, particularly for the region $|l| \lesssim 40°$.

2. Equipment and Observations

The observations were carried out in July 1974 during two continuous 16 h sessions, using the east–west fan beam of the Molonglo radio telescope. Spectral analysis was performed using an analogue filter bank consisting of 10 contiguous 30 kHz filters, whose outputs were continuously compared with that of a wide-band channel. Full details of the spectral analysis system and its calibration have been given elsewhere (Batty 1976). The entire region of the galactic equator accessible to the Molonglo telescope, from $l = 190°$ ($\alpha_{1950} \sim 06^h05^m$, $\delta_{1950} \sim +20°$) through $l = 360°$ to $l = 56°$ ($\alpha_{1950} \sim 19^h33^m$, $\delta_{1950} \sim +20°$) was covered, with the exception of several short periods of $\sim$10 min.

All the observations were made in an on/off source mode, the 'on' spectra being obtained at $b = 0°$, the reference spectra at positions at least 6° in declination away from the galactic equator. To increase stability, successive integration periods, which alternated between on and off positions, were each 10 min in time (and hence in right ascension). In order to follow the galactic equator during the on periods, the position of the aerial was stepped periodically, so that the maximum deviation of the centre of the beam from $b = 0°$ was always less than 1°. Successive alternating on/off periods were interchanged in the two sessions, so that a full coverage was obtained.

While re-positioning the aerial, electrical interference was found to be excessive (the aerial is normally stationary during observations in the cross mode). The data obtained during this period were rejected in later analysis. Approximately 30% of the total data were deleted in this way.

Since the sky brightness temperature near the galactic equator was generally higher than the reference regions, the total system temperature was not constant during the corresponding on and off periods, the variation being $<25\%$ everywhere except for a single 10 min period near $l = 0°$. The small residual nonlinear responses in the detectors were corrected in the analysis using independently determined calibrations. The maximum correction applied for the above level variation was $<0{\cdot}1\%$ of the system temperature.

The observations covered a total radial velocity range of about $\pm 100\ \mathrm{km\,s^{-1}}$. The local oscillator frequency was fixed, with the filter bank centred on the expected H 252α line rest frequency of 408·496 MHz, and hence no allowance was made for local standard of rest corrections, which amounted to about $\pm 20\ \mathrm{km\,s^{-1}}$. Consequently, the frequency corresponding to zero radial velocity varied with galactic longitude.

The brightness temperature scale was calibrated by using the known solid angle of the antenna beam together with observations of four calibration sources whose flux densities at 408 MHz were accurately tied to the Wyllie (1969) scale.

In the subsequent analysis, the samples were averaged over periods of 10 min to produce the on and off responses, and for each on period the nearby off responses were then subtracted to produce the final spectra. Linear baselines (at most several kelvins across the observed band) were then removed for convenience. Over the range of galactic longitude observed, 77 independent spectra were obtained. Since the galactic longitude is not a linear function of right ascension, the effective resolution of the observations varied with position. Near $l = 190°$ and 50° (the limits of the search) the resolution in l was $\sim$5°, whilst near $l = 300°$ the resolution was $\sim$1°.

3. Experimental Results

No significant spectral features were observed, apart from several isolated deflections which were all traced to instrumental effects. The calculated and measured r.m.s. noise levels in the final spectra agreed well, indicating that no other instrumental effects comparable with the noise fluctuations were present. On this basis a limit to the observed emission can be assigned. A 5σ deflection for one channel was about 0·6–0·9 K, depending on longitude. It is more difficult to assign a limit to the integrated line emission, where the velocity extent is unknown. Since the baselines have a fairly limited velocity extent in both directions, a genuine feature broadly extended in velocity is, by itself, indistinguishable from a baseline curvature. Thus any limit is only applicable to features less than, say, ~ 100 km s^{-1} in extent. However,

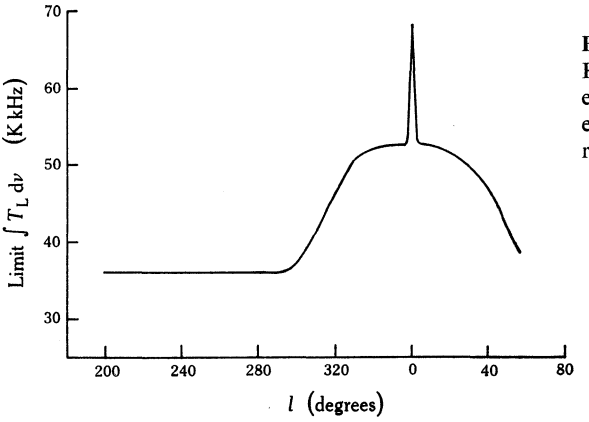

Fig. 1. Upper limits for integrated H 252α line emission near the galactic equator ($b = 0°$), observed with the east–west fan beam of the Molonglo radio telescope.

most of the H 166α features detected by Matthews *et al.* (1973) have a lesser velocity dispersion, a typical half-power width being 40 km s^{-1}. This restriction is therefore not unreasonable, even though some other broad emission features similar to those found by Gordon and Cato (1972) may be too wide to be unambiguously identified. For features having half-power widths $\lesssim 50$ km s^{-1} the upper limit was assumed to be a 5σ deflection for one channel multiplied by the width of two channels, and is shown in Fig. 1.

Although no obvious instrumental effects were evident in the spectra, a closer examination over the range $350° \lesssim l \lesssim 40°$ suggested that a slight curvature was present. Since this curvature was in the same sense as might be expected of very broad emission features having integrated line intensities comparable with the limits set above, it was desirable to check the validity of such features. Some of the spectral features of interest are expected to originate in the central thermal component of the galactic medium (i.e. $|l| \lesssim 40°$), and it is therefore useful to compare mean spectra observed at positions where a substantial thermal component is present with those at which little or no line emission would be expected. The procedure described below was used to estimate the thermal continuum contribution for two comparison regions. The important quantity in this comparison is the relative thermal contribution of the two regions rather than the actual thermal brightness temperatures. If the observed curvature is instrumental in origin, that is, produced by gain variations

across the receiver bandpass, the magnitude of such features should depend only on the total system temperature and the difference in continuum brightness temperature between the regions used to obtain the original on and off spectra.

The spectra at 20 positions over the range 327° to 46°, where the mean thermal brightness temperature was estimated to be 43 K, were averaged. This was repeated for 10 other positions in the range 309° to 321°, where the mean thermal brightness

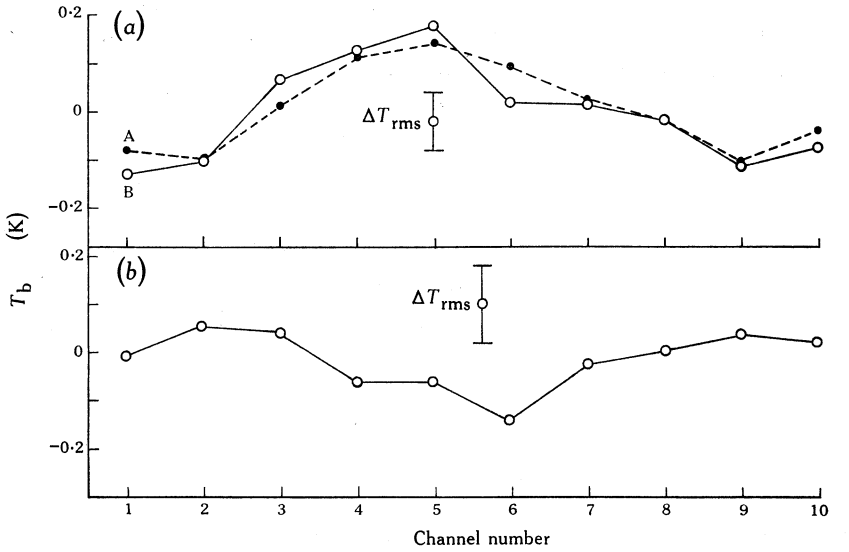

Fig. 2. Correction for instrumental baseline. The spectra A and B in (*a*) are averages at positions of estimated low and high continuum thermal brightness temperatures T_b respectively. The derived spectrum in (*b*) is the difference B–A after scaling A by a factor applicable if the curvature was due entirely to instrumental effects. The calculated r.m.s. fluctuations are indicated. No evidence of line emission is present.

temperature was only 4·5 K, but the *total* continuum temperature difference was still appreciable. The two mean spectra, designated B and A respectively, are shown in Fig. 2*a*. The latter spectrum was scaled by a factor corresponding to that expected if the curvature was due entirely to receiver bandpass effects and then subtracted from the former. The resulting spectrum is shown in Fig. 2*b*. There is no evidence of significant integrated line emission, and the uncertainties in the linearity corrections are comparable with the r.m.s. noise fluctuations. It was concluded that the residual curvature is consistent with instrumental causes. Using a similar criterion as before, a limit of ~25 K kHz was obtained for the integrated line emission in the mean difference spectrum of Fig. 2*b*.

4. Analysis of Results: General Method

In the following discussion, reference will be made to various components of the interstellar medium, and the following nomenclature has been employed:

(i) The interstellar medium thought to exist throughout the Galaxy, and whose general properties (usually in terms of a two-phase model) have been deduced by various methods, including 21 cm hydrogen line and pulsar dispersion studies, will be referred to as the *general interstellar medium.*

(ii) The distinct region of thermal emission near the galactic equator generally confined to the range $|l| \lesssim 40°$ will be referred to as the *central thermal component*. This component may not be characteristic of the interstellar medium in the remainder of the Galaxy and may in fact not consist of a true 'distributed' medium.

The observed upper limits for H 252α line emission may be used to deduce physical properties of the interstellar medium along the line of sight. This may be done in two ways: firstly, the results may be compared directly with the line intensities predicted by models of the general interstellar medium (e.g. Shaver 1975); secondly, if an estimate can be made for the continuum thermal brightness temperature of the ionized gas near the galactic equator, the upper limit for the line to continuum ratio leads to a lower limit for the electron temperature of the gas and, if non-LTE considerations are important, to an estimate for the electron density along the line of sight. The method of comparing line and thermal continuum emission has been employed by Gottesman and Gordon (1970), Jackson and Kerr (1971, 1975), Matthews *et al.* (1973) and Hirabayashi (1974) to calculate electron temperatures.

If the optical depth is small and the LTE approximation is valid then the line emission from the medium will be given by the equation (Pedlar and Davies 1972)

$$\frac{\int T_L \, dv}{T_c} = \frac{3{\cdot}12 \times 10^{-12} \nu^{2{\cdot}1} T_e^{-1{\cdot}15}}{a(\nu, T_e)\{1 + N(\mathrm{He})/N(\mathrm{H})\}}, \tag{1}$$

where the left-hand side represents the integrated line to continuum ratio, ν is the frequency (Hz), T_e is the electron temperature (K), $a(\nu, T_e) \approx 1$ and the ratio $N(\mathrm{He})/N(\mathrm{H}) \approx 0{\cdot}1$. Since the line to continuum ratio increases with decreasing temperature, the temperature inferred from any observations must be a *lower* limit for the *hottest* component present.

Alternatively, if values for both the continuum thermal brightness temperature and the electron temperature are assumed, application of non-LTE theory leads to lower limits for the electron density along the line of sight, since increasing density leads to decreasing line enhancement, at least for the range of conditions assumed here. Both methods of analysis will be considered.

It should be emphasized that the upper limits to line emission inferred from the present observational results are conservative in that they include any emission from 'normal' HII regions covered in the search, whereas the following analysis applies only to the 'unresolved' background.

5. Comparison with Models of the General Interstellar Medium

Table 1 summarizes the properties of the 'hot' (D) and 'cold' (E) components of a typical model of the general interstellar medium, considered by Shaver (1975). These values lead to the line and continuum characteristics given as the 'observable parameters' in the table. For comparison with the upper limits derived in the present work, it is necessary to take into account the expected spatial distribution of the two components. It is expected that a strong correlation should exist between observed neutral hydrogen features and recombination line emission from the same spatial regions. HI observations suggest that emission from both components should be restricted mainly to a region several degrees about the galactic equator, with a cosec $|b|$

dependence at higher latitudes. Because of the fairly broad declination beamwidth of the east–west fan beam, and the on/off mode of observation, it is unlikely that the broadest structural feature (i.e. the expected peak near $b = 0°$) would be resolved, or that no line emission would be present at the reference positions. In addition, these two effects are not independent, since the angle ϕ between the fan beam major axis

Table 1. Properties of model plasma clouds

For the typical model considered by Shaver (1975), with the indicated values of the electron temperature T_e, electron density N_e, path length L, r.m.s. turbulent velocity V_{rms}, continuum emission measure E and H252α line width $\Delta\nu$, the results for the 408 MHz continuum brightness temperature $T_{b,c}$, the peak line temperature $T_{b,L}$ and the integrated line temperature $\int T_L \, d\nu$ are as shown

Cloud component	Cloud properties						Observable parameters		
	T_e (K)	N_e (cm^{-3})	L (kpc)	V_{rms} ($km\,s^{-1}$)	E ($pc\,cm^{-6}$)	$\Delta\nu$ (kHz)	$T_{b,c}$ (K)	$T_{b,L}$ (K)	$\int T_L \, d\nu$ (K kHz)
D	10^3	0·05	10	10	25	20	1·2	0·07	1·5
E	20	0·05	1	10	2·5	20	0·5	2·6	51

and the galactic equator is a function of galactic longitude. Restricting the range of interest to those longitudes where $\phi \geqslant 45°$ (i.e. $270° \lesssim l \lesssim 330°$) and assuming that the expected line emission has an approximately gaussian distribution about $b = 0°$ with a half-power width of 1° to 6°, then the observed upper limits should be multiplied by a factor of 2–4 to be compared with that expected on the basis of the model. The neutral hydrogen profiles of McGee *et al.* (1966) near $b = 0°$ over these longitudes show a velocity extent of $\sim 100\,km\,s^{-1}$. For $l \lesssim 310°$ the profiles are fairly broad ($\sim 100\,km\,s^{-1}$) and centred near $-50\,km\,s^{-1}$, the integrated line intensities falling off fairly rapidly with $|b|$. For $310° \lesssim l \lesssim 330°$ the profiles are much narrower, and centred near $0\,km\,s^{-1}$, although the falloff with latitude is less abrupt. The velocity distribution of any recombination line emission should be similar to that of the HI features. Such values of velocity spread would be expected to affect the detectability of recombination lines to some extent with the limited velocity range of the present observations, and the calculated upper limits for $\int T_L \, d\nu$ should probably be raised by a factor $\lesssim 2$. Taken together, these considerations suggest that the observed upper limits should be multiplied by a factor of about 4–8 for comparison with the model predictions over this range of longitude.

By averaging the observed H252α spectra over a wider range of longitudes, an improvement in signal to noise ratio of ~ 6 over the single profiles was obtained. Fig. 3 shows the mean profile averaged over the range $268°{\cdot}5 \lesssim l \lesssim 324°{\cdot}6$. The expected r.m.s. noise level is $\sim 0{\cdot}022$ K, which corresponds to an upper limit of ~ 7 K kHz for the integrated line intensity. No significant line emission is present, although the curvature of the spectrum could be just consistent with a broad emission feature of this magnitude if the baseline were shifted downwards by $\sim 0{\cdot}02$ K. However, the magnitude of the curvature, while comparable with the noise level, is consistent with the instrumental effects considered in Section 3. Applying the factor of 4–8 to the limit for $\int T_L \, d\nu$ gives values of about 25–50 K kHz. This is clearly much higher than the expected emission from component D, (i.e. a typical

'intercloud' medium at ~1000 K) but might be expected from component E, particularly if the temperature in this component were raised by a factor $\gtrsim 2$, as would be favoured by some other models of the interstellar medium (see e.g. Field *et al.* 1969; Hjellming *et al.* 1969*b*).

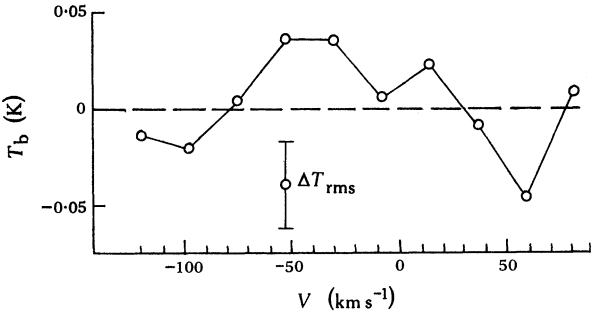

Fig. 3. Average H 252α spectrum obtained over the longitude range $268°\cdot5 \leqslant l \leqslant 324°\cdot6$ near $b = 0°$. V is the radial velocity relative to the local standard of rest for the H 252α transition. The expected r.m.s. noise level is ~0·022 K.

6. Central Thermal Component

(*a*) *Separation of Continuum Brightness Temperatures*

For the region of the galactic equator covering the range $|l| \lesssim 40°$, the continuum brightness temperature of the thermal component is considerably higher than at other galactic longitudes. If estimates of the thermal continuum brightness temperature in the direction of the present observations are made, then upper limits for the line to continuum ratios lead directly to lower limits for the electron temperature of the hottest component present, even if the gas is not in LTE. A separation of the continuum emission into its thermal (T) and nonthermal (NT) constituents is therefore required. The usual method of separation is to fit the total observed continuum temperature at each point to an expression of the form

$$T_b(\nu) = T_b(\mathrm{T}) + T_b(\mathrm{NT}) = C_1 \nu^{\beta_T} + C_2 \nu^{\beta_{NT}}, \qquad (2)$$

where β_T and β_{NT} are the thermal and nonthermal spectral indices and C_1 and C_2 are constants. In addition, correction for optical depth effects at low frequencies may be required.

Values for $T_b(\mathrm{T})$ were estimated by Matthews *et al.* (1973) from the maps of Altenhoff *et al.* (1970) and were used to derive electron temperatures of ~6000 K for the line-emitting gas from their H 166α recombination line observations. These estimates were criticized by Gottesman and Gordon (1972), who considered the thermal continuum component to be much lower. They argued that the expression (2) above for $T_b(\nu)$ may not be sufficiently representative of the true spectrum, and that the procedure is unduly sensitive to experimental uncertainties and inaccuracy in the assumed value for β_{NT}. Hirabayashi (1974) and Jackson and Kerr (1975), using independent analyses, obtained values for the electron temperature roughly similar to that of Matthews *et al.* (i.e. $\gtrsim$3000 K). It is shown in the present analysis

that, although there is still some uncertainty regarding the magnitude of thermal brightness temperatures, there is reason to believe that the values estimated by Matthews *et al.* should be substantially correct.

(*b*) *Thermal Maps of Large* et al. (*1961*) *and Mathewson* et al. (*1962*)

In earlier work, Large *et al.* (1961) fitted thermal and nonthermal temperatures near the galactic equator for the range $350° \lesssim l \lesssim 55°$, using their own 408 MHz data and the surveys of Hill *et al.* (1958) and Westerhout (1958). Mathewson *et al.* (1962) published similar maps for the range $260° \lesssim l \lesssim 88°$ from analyses using their own 1440 MHz data, those of Hill *et al.* and Large *et al.*

For the purposes of estimating thermal brightness temperatures in the present work, the maps of Large *et al.* (1961) and Mathewson *et al.* (1962), having a resolution of $\sim 1°$, would be suitable, as the maximum resolution of the present search is $\sim 1°$ (determined by the integration period). However, it should be established that the thermal temperatures have not been significantly overestimated. For this purpose, the possible systematic errors inherent in the earlier analyses were examined in detail.

Calibration Errors. The consistency of the temperature scales in the surveys used was examined by comparing the adopted flux densities for the calibration sources with the recent values given by Baars and Hartsuijker (1972) and Wills (1973). Typical thermal separations were performed with both the original and revised temperature scales, assuming that the adopted values for β_T and β_{NT} were correct. No significant difference was found in the results.

Spectral Indices. Calculations showed that no significant bias was caused by the assumption of a thermal spectral index of $-2{\cdot}0$. However, β_{NT} is less precisely known and is frequency dependent to some degree. A mean value of $-2{\cdot}6$ was adopted by Large *et al.* (1961) and Mathewson *et al.* (1962), whilst Matthews *et al.* (1973) assumed a value of $-2{\cdot}9$ at higher frequencies. Komesaroff (1961) obtained a value of $-2{\cdot}6 \pm 0{\cdot}1$ over the range 19·7–1390 MHz, and found that it was fairly constant throughout. Jones and Finlay (1974) found a value of $-2{\cdot}72$ to be appropriate at $l = 347°$. Similar fittings at 10 points over the range $310° < l < 342°$ at $b = \pm 4°$, using the results of Hill *et al.* (1958), Mathewson *et al.* (1962), Komesaroff (1966) and Price (1970) give a mean value for β_{NT} of $-2{\cdot}63 \pm 0{\cdot}04$ (standard error). The effect of assuming too positive a value for β_{NT} is to underestimate the thermal component. Further fittings near $l = 323°$ using additionally the maps of Hill (1968) and Jones and Finlay (1974) produced no significant evidence of a latitude dependence of β_{NT}.

Other Factors. (i) Resolution differences should not have produced any significant bias in the results, since all the surveys used had beamwidths of 47′ to 50′ arc, except that of Westerhout (1958). However, this survey was used only by Large *et al.* (1961), and their analysis took account of such effects. (ii) The possibility of non-negligible optical depth at 85 MHz has been discussed by Mathewson *et al.* (1962). The results of Dulk and Slee (1972) indicate that optical depths of $>0{\cdot}5$ at 80 MHz may be characteristic of the regions of interest, and this could affect the 'complete mixing' model. However, the fact that Mathewson *et al.* found that analyses using *either* 85 or 408 MHz data gave essentially identical results would appear to justify their assumptions.

Despite the above results, it is still possible that the basic model assumed for the continuum emission was not correct. It may well be that a more complex model involving variation of β_{NT} with frequency, latitude or longitude is necessary, since the spectral characteristics of any distributed components may depend on their galactic distribution. In such a case multiparameter models would probably be limited by observational uncertainties.

As an independent check on these analyses, thermal temperatures derived from the earlier surveys were compared with those obtained by Matthews *et al.* (1973). The values obtained for T_b(T) at the 13 positions observed by Matthews *et al.* were compared with those from the analysis of Mathewson *et al.* (1962) at $b = 0°$. The former values exhibit a greater dispersion, as might be expected because of the higher resolution. However, the mean values of 6·0 and 6·2 K respectively at 1·4 GHz are in good agreement. In order to correct for large-scale resolution effects, it is estimated that the latter value should be scaled upwards by $<20\%$.

As a final check, an independent separation using the maps of Altenhoff *et al.* (1970) was attempted. For this purpose, latitude cuts were made at 10 positions, including the longitudes $l = 13°{\cdot}5$, $25°{\cdot}1$ and $29°{\cdot}5$ observed by Matthews *et al.* (1973), brightness temperatures being estimated for $-1°{\cdot}5 \leqslant b \leqslant 1°{\cdot}5$. Providing enough data points are available, it is in principle possible to fit both T_b(T) and T_b(NT) at each point, as well as β_{NT} and baselevels for all three maps simultaneously. Although reasonable values for β_{NT} (about $-3{\cdot}0$) and baselevels were obtained, several facts were apparent: (i) the scarcity of reliable 5 GHz contour levels severely limited the accuracy of the procedure; (ii) the convergence of the solutions was often extremely poor when the data were subdivided; (iii) the values of T_b(T) obtained were sometimes much lower than those estimated by Matthews *et al.*; (iv) systematic discrepancies in the fitted thermal temperatures, apparent as negative values near the extreme limits of b, were sometimes obtained.

The above effects, particularly (iv), suggest that the assumed model may be deficient, and that more reliable continuum measurements are desirable. In view of this, the acceptance of a reliable thermal temperature scale should still be treated with caution. Whilst it appears that the 'background' thermal temperatures derived in the earlier analyses are essentially valid for the resolution attained (i.e. within, say, 20–30%) it is apparent that more work is necessary in this area. For the present investigation the thermal temperature values derived by Large *et al.* (1961) and Mathewson *et al.* (1962) were tentatively adopted and used in the following analysis.

(*c*) *Estimation of Fan Beam Thermal Temperatures*

The brightness temperatures from the thermal maps of Mathewson *et al.* (1962) were first scaled to 408 MHz. These results were used for $l < 0°$ and those of Large *et al.* (1961) for $l \geqslant 0°$. At each observed position, a cut was made at the appropriate angle on the thermal maps and the estimated temperatures were convolved with a gaussian function to produce an effective resolution matching that of the aerial beam. A similar convolution was performed for the off positions, and the value of ΔT_b(T), the difference in thermal full beam brightness temperature between the on and off positions, was found for each longitude. The values of ΔT_b(T) thus calculated are shown in Fig. 4. For $l \lesssim 260°$ the value is close to zero. The uncertainty in the temperature is about ± 5 K relative to the original maps.

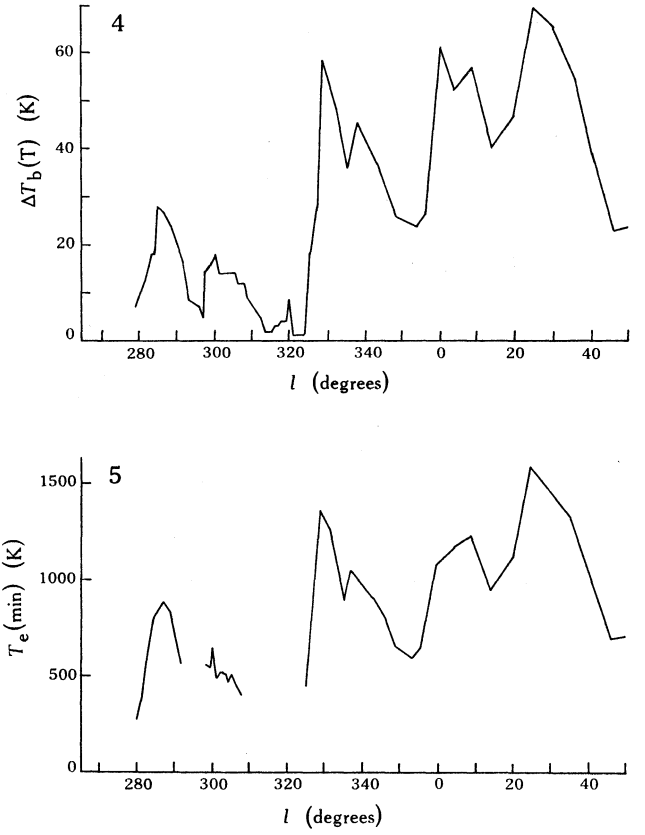

Fig. 4. Calculated differences ΔT_b(T) in 408 MHz thermal fan beam brightness temperatures between $b = 0°$ and the reference positions.

Fig. 5. Lower limits for the electron temperature T_e(min) of the hottest component present near $b = 0°$, calculated using equation (1) and the data from Figs 1 and 4.

(d) Derivation of Physical Parameters: LTE Analysis

If the medium along the line of sight is optically thin and close to LTE, the values of ΔT_b(T) obtained above may be combined with the corresponding limits for $\int T_L \, dv$ to deduce lower limits for the electron temperature of the hottest component present. Dulk and Slee (1972) measured 80 MHz absorption in the direction of known supernova remnants and, for $|l| < 40°$, a mean absorption of $0{\cdot}20$ kpc^{-1} was obtained. For a maximum path length through the Galaxy of $\sim$15 kpc, this corresponds to an optical depth of $\lesssim 0{\cdot}1$ when scaled to 408 MHz, justifying the assumption of small optical depth along the line of sight. Considering this together with the thermal brightness temperatures of Mathewson *et al.* (1962) leads to the conclusion (from the continuum data alone) that the electron temperature in the absorbing medium should be high, that is, $\gtrsim$1000 K. Applying equation (1) and putting $T_c = \Delta T_b$(T), with $\int T_L \, dv$ equal to the corresponding limit for integrated line brightness temperature, a value of the lower limit for the electron temperature T_e(min) was calculated at each position where ΔT_b(T) was estimated to be greater than 10 K. The

values are plotted in Fig. 5, and are 1500–1600 K at a few positions. In addition, the upper limit deduced from Fig. 2 was analysed in a similar way, yielding a value of ~1750 K.

On the basis of the preceding results, line emission from regions with electron temperatures in the approximate range 1000–2000 K should have been detectable. The mean spectrum of Fig. 2*b* shows no indication of line emission, even at a lower significance level. On the other hand, the non-detection of line emission is still consistent with electron temperatures of 4000–6000 K, as estimated by Matthews *et al.* (1973) and Jackson and Kerr (1975). An electron temperature of ~6000 K would correspond to ~0·15 kHz for $\left(\int T_L \, dv\right)/T_c$, or to ~6 K kHz for $\int T_L \, dv$ (for $\Delta T_b(T) \approx 40$ K). Detection of such emission would require an increase in sensitivity by a factor of about 4–5 for the LTE case.

(e) Non-LTE Effects

Modification of the above limits by non-LTE effects is now examined. Consider first the case of a hot ($\geqslant$1000 K) component alone, neglecting the effects of any ambient radiation fields. For small optical depth the approximate relationship for a constant density model is (Brocklehurst and Seaton 1972)

$$Y = b\{1 + \tfrac{1}{2}(1-\beta)\tau_c\}, \tag{3}$$

where Y is the line enhancement factor, b is the departure coefficient, β is the stimulated emission term defined by Goldberg (1966) and τ_c is the continuum optical depth. The tables of Brocklehurst (1970) were used to obtain values for b_n and C_n (and hence β) for $N_e \geqslant 10$ cm^{-3} and $T_e = 2500$ and 5000 K. Near $n = 250$, C_n is a fairly linear function of $\log N_e$ for $N_e \gtrsim 1$ cm^{-3} (see e.g. Fig. 2 of Hoang-Binh 1968), and is only weakly dependent on T_e. For $1 \lesssim N_e \lesssim 10$ cm^{-3} and $T_e \gtrsim 2500$ K, values were therefore extrapolated from the above tables. For $T_e = 1000$ K, departure coefficients were taken from Dupree (1972). The continuum optical depth τ_c was calculated for peak 400 MHz thermal continuum brightness temperatures of 50 and 100 K near the galactic equator. For $1000 \leqslant T_e \leqslant 5000$ K, the value of τ_c lies in the range $0{\cdot}1 \leqslant \tau_c \leqslant 0{\cdot}01$ with the above values. Using these data, the ratio $\left(\int T_L \, dv\right)/T_c$ was calculated for various cases, and the results are plotted in Fig. 6*a*.

An approximate lower limit for N_e may be set by consideration of the emission measure E along the line of sight. From the relationship of Mezger and Henderson (1967),

$$\tau_c \approx 8{\cdot}2 \times 10^{-2} \, a(v, T_e) \, T_e^{-1{\cdot}35} \, v^{-2{\cdot}1} \, E \tag{4}$$

(with T_e in K, v in GHz and E in pc cm^{-6}), the above cases correspond to emission measures of $\gtrsim$1000 pc cm^{-6}. For a path length L through the emitting matter of $\lesssim$10 kpc, this sets a lower limit of ~0·3 cm^{-3} for N_e, and this is indicated in Fig. 6*a*, together with the observed upper limit for $\left(\int T_L \, dv\right)/T_c$. These two lines then define the possible area of solution. For a peak thermal brightness temperature of ~100 K (a typical case), the value for N_e is $\gtrsim$1 cm^{-3} if $T_e = 5000$ K, whilst $N_e \gtrsim 10$ cm^{-3} if $T_e = 2500$ K. Since the line enhancement decreases with increasing electron density, an 'observed' value of Y is characterized by the maximum densities along the line of sight (see e.g. the models of Hjellming *et al.* 1969*a*). These values are thus consistent with the 'most probable' model proposed by Matthews *et al.* (1973), having a local average $\langle N_e \rangle \sim 10$ cm^{-3} and $T_e \approx 6000$ K.

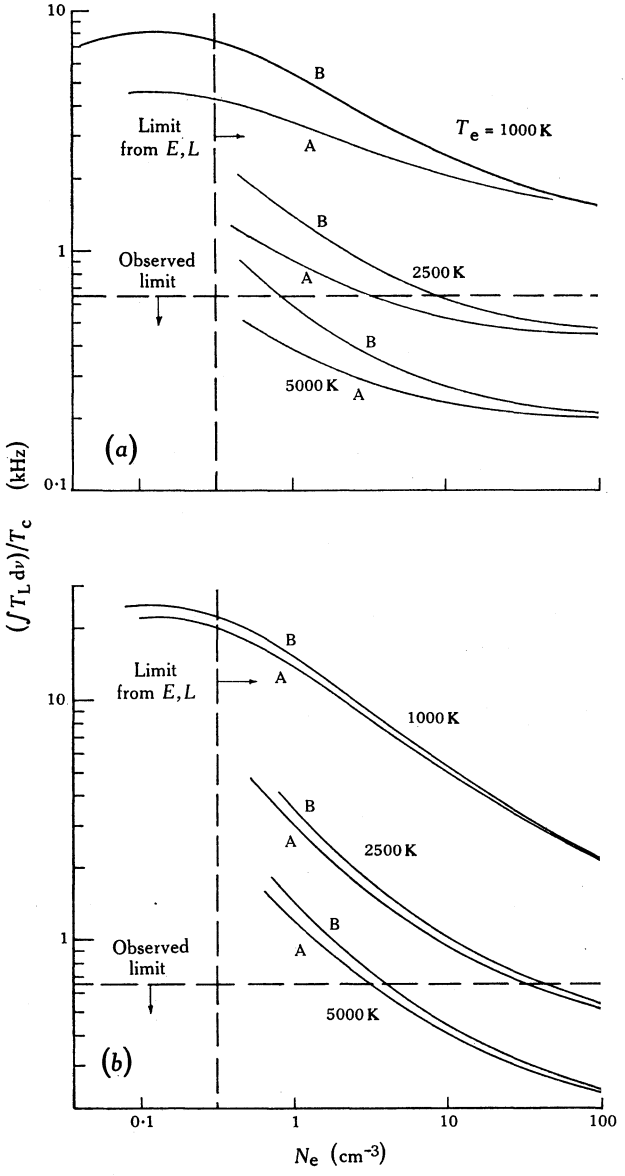

Fig. 6. Calculated H 252α line to continuum ratios for (*a*) various models of the central thermal component alone, and (*b*) the same models but including the effect of a nonthermal radiation field of total brightness temperature 200 K. The models A and B correspond to thermal continuum brightness temperatures of 50 and 100 K respectively at 408 MHz. The nonthermal emission included in (*b*) is either well mixed with the thermal emission or is situated so that half lies behind and half in front of the thermal region.

Consider now the case where the effect of the galactic radiation field is included. For this purpose the general equation for the line temperature given by Shaver (1975) is applicable:

$$T_L = T_0\left(\exp(-\tau_c)\{\exp(-\tau_L)-1\}\right) + T_e\left(\frac{[b_m\tau_L^* + \tau_c][1-\exp\{-(\tau_L+\tau_c)\}]}{\tau_L+\tau_c} - \{1-\exp(-\tau_c)\}\right) + T_s\left(\frac{1-\exp\{-(\tau_L+\tau_c)\}}{\tau_L+\tau_c} - \frac{1-\exp(-\tau_c)}{\tau_c}\right), \quad (5)$$

where T_0 is the background temperature, T_s is the temperature due to the distributed nonthermal emission and τ_L is the optical depth in the line. The values of τ_L and τ_c are conveniently given by

$$\tau_L = \frac{523\,E}{\nu\Delta V_L T_e^{5/2}} b_n\left(1 - \frac{20\cdot 8\,T_e}{\nu}\frac{d(\ln b_n)}{dn}\right), \qquad \tau_c = \frac{0\cdot 0314\,E}{\nu^2 T_e^{3/2}}\left(1\cdot 5\ln T_e - \ln(20\cdot 2\,\nu)\right) \quad (6)$$

for α lines, where ΔV_L is in km s^{-1} and it is assumed that $N(H^+) = 0\cdot 9 N_e$ and $n \gg 1$. In order to estimate T_0 and T_s (both taken to be due to the galactic nonthermal field), it was assumed that the thermal and nonthermal components were at the same *average* distance. However, the distribution of each along the line of sight is also an unknown parameter. Two distributions were considered: one with half the nonthermal emission behind the thermal region, half in front; the other with both components uniformly mixed. A representative total brightness temperature of 200 K at 400 MHz was assumed for the nonthermal field; both configurations then gave almost identical solutions. The behaviour of the models is shown in Fig. 6*b*. Significant line enhancement is predicted, and the solutions are reasonably independent of the assumed thermal brightness temperature. In all cases the line to continuum ratio increases with decreasing density. For $T_e = 5000$ or 2500 K, the observed upper limit would imply that the electron density must be at least approximately 3 or 30 cm^{-3} respectively.

7. Conclusions

(i) The upper limits over the range $270° \lesssim l \lesssim 325°$ just admit the model of Shaver (1975) for a cold cloud component having $T_e \geqslant 20$ K, indicating that such models do not seriously overestimate the expected recombination line radiation at this frequency. No conclusions can be drawn concerning the validity of the hot component model. An improvement in sensitivity of only about 2–3 might be needed in order to detect the cold cloud emission, if the model is correct. A search using, for example, the Parkes 64 m radio telescope at this frequency in the direction of known neutral hydrogen concentrations might thus be fruitful. A position of relatively high HI line temperatures and narrow velocity dispersion would be the most logical place for such a search. In this respect, positions near $l \approx 315°$ to 323° (where the central thermal component is also small) would probably be most favourable.

(ii) Provided that the estimates of thermal brightness temperatures for $|l| \lesssim 40°$ are substantially correct, meaningful limits for the physical parameters along the line of sight in such directions may be made. It should, however, be emphasized that some doubt still exists about the magnitude of the thermal continuum temperatures, and more work is necessary in this area. Assuming the thermal temperatures to be correct, and LTE to apply along the line of sight, single observations of regions $<5°$ in extent yield lower limits for the electron temperature in the hottest component. Lower limits of ~ 1600 K are obtained for a few positions, whilst average spectra over the range $330° \lesssim l \lesssim 45°$ imply lower limits of ~ 1750 K.

(iii) Estimation of probable non-LTE effects in the medium lead to lower limits for the electron density along the line of sight, provided an electron temperature is assumed. In addition, the line enhancement may be significantly affected by the presence of the galactic nonthermal radiation field at this frequency.

Simple consideration of the peak *continuum* thermal brightness temperatures near $b = 0°$ and the probable path length through the Galaxy suggest that the electron density should be $\gtrsim 0{\cdot}3\ \mathrm{cm}^{-3}$ for $|l| \lesssim 40°$. For electron temperatures of 5000 K or 2500 K in the central thermal component, consideration of non-LTE effects for the H 252α line indicates that peak electron densities along the line of sight should be $\gtrsim 1$ or $\gtrsim 10\ \mathrm{cm}^{-3}$ respectively. The addition of a typical nonthermal field might raise these estimates by a factor of ~ 3.

(iv) The temperature limits derived here are consistent with the values of 3000–6000 K derived by Matthews *et al.* (1973), Hirabayashi (1974) and Jackson and Kerr (1975), but probably not with earlier estimates of 1000–2000 K. In addition, the lower limits for electron density support the conclusions reached by most of these authors, namely that the observed emission probably arises in complexes of low surface brightness HII regions, rather than the hot component of the general interstellar medium. Pankonin (1975) suggests similar densities for the medium along the line of sight in the direction of his 248α observations near G44·2+0·0. Interpretations of line spectra by the same author, Chaisson (1974) and Downes and Wilson (1974), taken in the direction of supernova remnants, have led to similar conclusions, although Cesarsky and Cesarsky (1973*a*, 1973*b*) suggest cold clouds as the probable source. A more accurate assessment of the background thermal continuum component would help to resolve the remaining uncertainties.

In addition to determining the properties of the interstellar medium, the determination of distributed background line emission can be important in the analysis of low frequency recombination line observations of HII regions, where the contamination of the observed nebular profiles due to the galactic background is not known.

Acknowledgments

The author is grateful to Professor B. Y. Mills and Dr W. M. Goss for helpful discussion. The receipt of a Commonwealth Postgraduate Studentship during the earlier part of this work is gratefully acknowledged. Research at the Molonglo Observatory is supported by the Australian Research Grants Committee, the Sydney University Research Grants Committee and the Science Foundation for Physics within the University of Sydney.

References

Altenhoff, W. J., Downes, D., Goad, L., Maxwell, A., and Rinehard, R. (1970). *Astron. Astrophys. Suppl.* **1**, 319.
Baars, J. W. M., and Hartsuijker, A. P. (1972). *Astron. Astrophys.* **17**, 172.
Batty, M. J. (1976). Ph.D. Thesis, University of Sydney.
Brocklehurst, M. (1970). *Mon. Not. R. Astron. Soc.* **148**, 417.
Brocklehurst, M., and Seaton, M. J. (1972). *Mon. Not. R. Astron. Soc.* **157**, 179.
Cesarsky, C. J., and Cesarsky, D. A. (1971). *Astrophys. J.* **169**, 293.
Cesarsky, D. A., and Cesarsky, C. J. (1973*a*). *Astrophys. J.* **183**, L143.
Cesarsky, D. A., and Cesarsky, C. J. (1973*b*). *Astrophys. J.* **184**, 83.
Chaisson, E. J. (1974). *Astrophys. J.* **189**, 69.
Downes, D., and Wilson, T. L. (1974). *Astron. Astrophys.* **34**, 133.
Dulk, G. A., and Slee, O. B. (1972). *Aust. J. Phys.* **25**, 429.
Dupree, A. K. (1972). *Astrophys. J.* **173**, 293.
Field, G. B., Goldsmith, D. W., and Habing, H. J. (1969). *Astrophys. J.* **155**, L149.
Goldberg, L. (1966). *Astrophys. J.* **144**, 1225.
Gordon, M. A., Brown, R. L., and Gottesman, S. T. (1972). *Astrophys. J.* **178**, 119.
Gordon, M. A., and Cato, T. (1972). *Astrophys. J.* **176**, 587.
Gottesman, S. T., and Gordon, M. A. (1970). *Astrophys. J.* **162**, L93.
Gottesman, S. T., and Gordon, M. A. (1972). *Nature Phys. Sci.* **240**, 160.
Hill, E. R. (1968). *Aust. J. Phys.* **21**, 735.
Hill, E. R., Slee, O. B., and Mills, B. Y. (1958). *Aust. J. Phys.* **11**, 530.
Hirabayashi, H. (1974). *Publ. Astron. Soc. Japan* **26**, 263.
Hjellming, R. M., Andrews, M. H., and Sejnowski, T. J. (1969*a*). *Astrophys. J.* **157**, 573.
Hjellming, R. M., Gordon, C. P., and Gordon, K. J. (1969*b*). *Astron. Astrophys.* **2**, 202.
Hoang-Binh, D. (1968). *Astrophys. Lett.* **2**, 231.
Jackson, P. D., and Kerr, F. J. (1971). *Astrophys. J.* **168**, 29.
Jackson, P. D., and Kerr, F. J. (1975). *Astrophys. J.* **196**, 723.
Jones, B. B., and Finlay, E. A. (1974). *Aust. J. Phys.* **27**, 687.
Komesaroff, M. M. (1961). *Aust. J. Phys.* **14**, 515.
Komesaroff, M. M. (1966). *Aust. J. Phys.* **19**, 75.
Large, M. I., Mathewson, D. S., and Haslam, C. G. T. (1961). *Mon. Not. R. Astron. Soc.* **123**, 113.
McGee, R. X., Milton, J. A., and Wolfe, W. (1966). *Aust. J. Phys. Astrophys. Suppl.* No. 1.
Mathewson, D. S., Healey, J. R., and Rome, J. M. (1962). *Aust. J. Phys.* **15**, 354.
Matthews, H. E., Pedlar, A., and Davies, R. D. (1973). *Mon. Not. R. Astron. Soc.* **165**, 149.
Mezger, P. G., and Henderson, A. P. (1967). *Astrophys. J.* **147**, 471.
Pankonin, V. L. (1975). *Astron. Astrophys.* **38**, 445.
Pedlar, A., and Davies, R. D. (1972). *Mon. Not. R. Astron. Soc.* **159**, 129.
Price, R. M. (1970). *Aust. J. Phys.* **23**, 227.
Shaver, P. A. (1975). *Pramana* **5**, 1.
Westerhout, G. (1958). *Bull. Astron. Inst. Neth.* **14**, 215.
Wills, B. J. (1973). *Astrophys. J.* **180**, 335.
Wyllie, D. V. (1969). *Mon. Not. R. Astron. Soc.* **142**, 229.

Manuscript received 7 June 1976